Supporting Information For

Exploring the Cytotoxicity of Dinuclear Ru(II) *p*-cymene Complexes Appended N,N'-Bis(4-substituted benzoyl)hydrazines: Insights into the Mechanism of Apoptotic Cell Death

Arunachalam Abirami,[a] Rengan Ramesh,[a*] Devan Umapathy,[b] Antony Joseph Velanganni Arockiam,[b] Jan Grzegorz Małecki[c]

[a]Centre for Organometallic Chemistry, School of Chemistry, Bharathidasan University, Tiruchirappalli – 620 024, India.

[b]Molecular Oncology Laboratory, Department of Biochemistry, School of Life Sciences, Bharathidasan University, Tiruchirappalli – 620 024, India.

[c]Department of Crystallography, Institute of Chemistry, University of Silesia, 40-006,Katowice, Poland.

[*]Corresponding author [Tel: +91-431-2407053, Fax: +91-431-2407045, E-mail: ramesh_bdu@yahoo.com]

Contents

1. Materials and Methods

Best commercial-grade reactants and solvents were used for all the reactions. $RuCl_3.3H_2O$, benzoyl chloride, 4-chloro benzoyl chloride, 4-methoxy benzoyl chloride, hydrazine hydrate were purchased from Sigma Aldrich. Dimer ruthenium precursor $[(\eta^6\text{-}p\text{-cymene})RuCl_2]_2$ was prepared from the procedures as specified in the literature.[1-3] FT-IR spectra were recorded in the range of 4000–400 cm^{-1} with Perkin-Elmer 597 spectrophotometer. Electronic spectra were recorded in chloroform solution using CARY 300 Bio UV-visible Varian spectrometer. The NMR spectral studies were carried out on a Bruker 400 MHz spectrometer in presence of $CDCl_3$ solvent using tetramethylsilane (TMS) as internal reference. A Micro mass thermo-scientific LTQ XL mass spectrometer was used for High-Resolution Mass Spectrometry of the complexes. Single crystals of complexes **Ru_2H1** and **Ru_2H3** were grown by slow evaporation of a dichloromethane and petroleum ether solution at room temperature. A single crystal of suitable size was covered with Paratone oil, mounted on the top of a glass fibre, and transferred to a Bruker AXS Kappa APEX II single crystal X-ray diffractometer using monochromated MoK_α radiation (λ = 0.71073). Data were collected at 293 K. The structure was solved by direct methods using SIR-97 and was refined by the full matrix least-squares method on F2 with SHELXL-97.[4,5] Non-hydrogen atoms were refined with anisotropy thermal parameters. All hydrogen atoms were geometrically fixed and collected to refine using a riding model. Complex **Ru_2H1** and **Ru_2H3** were drawn with ORTEP and the structural data have been deposited at the Cambridge Crystallographic Data Centre: CCDC for complex **Ru_2H1** and **Ru_2H3** are **2181517** and **2181516** respectively. These data can be obtained free of charge from The Cambridge Crystallographic Data Center (CCDC) via http://ac.uk/data_request/cif.

2. Experimental procedures

Stability Analysis

UV-visible spectroscopy was employed to evaluate the stability of the complexes in a time-dependent manner. **Ru_2H1- Ru_2H3** were taken in a minimum amount of 1% DMSO and then diluted with PBS buffer to 1×10^{-3} M concentration. The hydrolysis profiles of the complexes were monitored by their electronic spectra over 72 h.[7]

The stability of the complexes Ru2H1- Ru2H3 was studied by ^{1}H NMR spectroscopy in DMSO(d_6)-D_2O (6:4) combination for 24 hours to examine the hydrolysis products. The representative complex (**Ru_2H3**) solution was prepared in DMSO-d_6, and its initial spectrum was recorded. Subsequently, D_2O was included, and the spectra were recorded again over the stated duration.[7]

Partition Coefficient Calculation(Log P)

The "shake-flask" technique was used to evaluate the lipophilicity of complexes **Ru_2H1- Ru_2H3** using octanol/water phase partitions. Double distilled water and analytical grade octanol (Sigma Aldrich) were used to produce octanol-saturated water and water-saturated octanol phases. Complexes (1 mg/mL; ethanol/water) have been prepared to 2, 4, 6, 8, and 10 µg/mL in water and alternately scaled to 2, 4, 6, 8, and 10 µg/mL in octanol, respectively. Equal volumes (50/50) of the complexes in the proper concentrations (4 mg/mL) have been shaken for 24 hours at ambient conditions. The water and organic fractions have been segregated and centrifuged when equilibrium was attained. Finally, UV-visible spectroscopy was used to determine the complex concentration in each phase.[8] The concentration of the sample solution was used to calculate the partition coefficients (log P) by adopting the equation,

Log P = log[(**Ru_2H1- Ru_2H3**)octanol/(**Ru_2H1- Ru_2H3**)water].

Cell culture

The cancer cell lines Lung (H460), Breast (SKBR3), Cervical (HeLa) and Liver (HepG2) were purchased from the National Centre for Cell Science (NCCS, Pune, India). Cell lines were grown in RPMI 1640, DMEM or DMEM/F12 medium supplemented with 10% FBS and 0.5% antibiotics in a humidified environment at 37° C under 5% CO2.

MTT assay

The cancer cells (1×10^4) were seeded in a 96-well plate. After 48 h, cells were incubated with different concentrations of compounds (**Ru_2H1-Ru_2H3**) for 48 h. The highest DMSO concentration used to dissolve the compounds was used as a control (Vehicle). After 24h, the medium was removed and washed with 1X PBS. Then 20µl of freshly prepared MTT solution (5mg/ml in PBS) and 180µl serum-free medium were added to the plates and incubated for 4 hours. After the incubation, the medium was removed, and 200µl of DMSO was added to dissolve the formazan crystals. The absorbance was measured using a microplate reader (BioRad, CA, USA) at 595 nm. Graph pad prism software (V9.3.1) was used to calculate the IC_{50} values.

Cell viability = Absorbance of treated * 100 / Absorbance of vehicle control

AO/EB staining

AO-EB dual staining assay was employed to examine the apoptotic morphology in cancer cells. 1 x 10^5 H460 cells were seeded in a 6-well plate. After 24h, the cells were treated with IC_{50} concentrations of compounds (**Ru_2H1-Ru_2H3**) for 48h. Following treatment, the culture medium was removed, and cells were washed with PBS. The cells were stained with AO (10µg/mL)/ EB (10µg/mL) for 20 minutes in the dark. The excess stain was removed by washing with PBS, and the cells were visualized under a fluorescent microscope at 20X magnification (Floid imaging station, Life Technologies, USA).

Hoechst 33342 staining

Hoechst 33342 staining was used to visualize the nuclear condensation process in apoptosis. 1 x 10^5 H460 cells were seeded in a 6-well plate. After 24h, the cells were treated with IC_{50} concentrations of compounds (**Ru_2H1-Ru_2H3**) for 48h. Following treatment, the culture medium was removed, and cells were washed with PBS. The cells were stained with Hoechst 33342 (5µg/mL) for 10 minutes in dark. The excess stain was removed by washing with PBS, and the cells were visualized under a fluorescent microscope at 20X magnification (Floid imaging station, Life Technologies, USA).

Reactive Oxygen Species (ROS) Assay

DCFDA is a cell-permeant dye and was used to evaluate the free radical production in compound-treated cells. 1 x 10^5 H460 cells were seeded in a 6-well plate. After 24h, the cells were treated with IC_{50} concentrations of compounds (**Ru_2H1-Ru_2H3**) for 48h. Following treatment, the culture medium was removed, and cells were washed with PBS. The cells were stained with DCFDA (10ug/mL) in the dark for 10 minutes. The excess stain was removed by washing with PBS, and the cells were visualized under a fluorescent microscope at 20X magnification (Floid imaging station, Life Technologies, USA).

Mitochondrial Membrane Potential (MMP)

Rhodamine-123 was used to visualize the integrity of the mitochondria in complex-treated cells. 1 x 10^5 H460 cells were seeded in a 6-well plate. After 24h, the cells were treated with IC_{50} concentrations of compounds (**Ru_2H1-Ru_2H3**) for 48h. Following treatment, the culture medium was removed, and cells were washed with PBS. The cells were stained with Rhodamine-123 (10µg/mL) for 15 minutes in the dark. The excess stain was removed by washing with PBS, and the cells were visualized under a fluorescent microscope at 20X magnification (Floid imaging station, Life Technologies, USA).

Western blot

H460 cells (3 x 10^5) were seeded in 6-well plates. After 24h, the cells were treated with IC50 concentrations of complex **Ru_2H3** for 48h. The total proteins were isolated by the RIPA lysis buffer method, and 50 µg of protein was subjected to SDS-PAGE for separation; consequently, the SDS-PAGE was electroblotted onto nitrocellulose membranes, and the membranes thus obtained were blocked with non-fat dry milk for 1 h at 37˚C. Then membranes were incubated overnight with specific antibodies anti-Cas9, anti-Bcl2, anti-Bax, anti-Cytochrome c, anti-pAkt, and anti-β-Actin. Further, the membranes were washed with TBST and incubated with ALP-conjugated secondary antibody (2 hrs at 37˚C). Then, washed with TBST thrice, and BCIP/NBT substrate was used to develop the blots. GelDoc™ XR+ (BioRad, CA, USA) was used for imaging and quantification of the blots.

Annexin V-FITC/PI staining by flow cytometry

The cells have been seeded in a 6-well plate (10^5 cells/well) and cultured at 37 °C for 24 hours. The cells were treated with IC_{50} doses of the complex (**Ru_2H3**) and incubated for 48 hours. Then, the cells were trypsinized, washed with PBS, and stained with annexin V-

FITC/PI according to the annexin V-FITC apoptosis detection kit. Finally, apoptosis induction has been assessed using a flow cytometer (SYSMEX, Japan). Flow Jo software has been used to analyze the results. The untreated cells were employed as a control group.

Statistical analysis

All the data was analyzed by GraphPad Prism version 9.3.1 software (GraphPad Software, San Diego, CA). The student's t-test was used to examine significant difference between two groups, and the one-way ANOVA test for multiple group comparisons were used to compare the groups. P values less than 0.05 were considered significant (*P < 0.05, **P < 0.01, ***P < 0.001, ****P<0.0001, ns – non-significant), and all the experiments were done in triplicates.

3. UV-vis spectra of complexes(Ru_2H1- Ru_2H3)

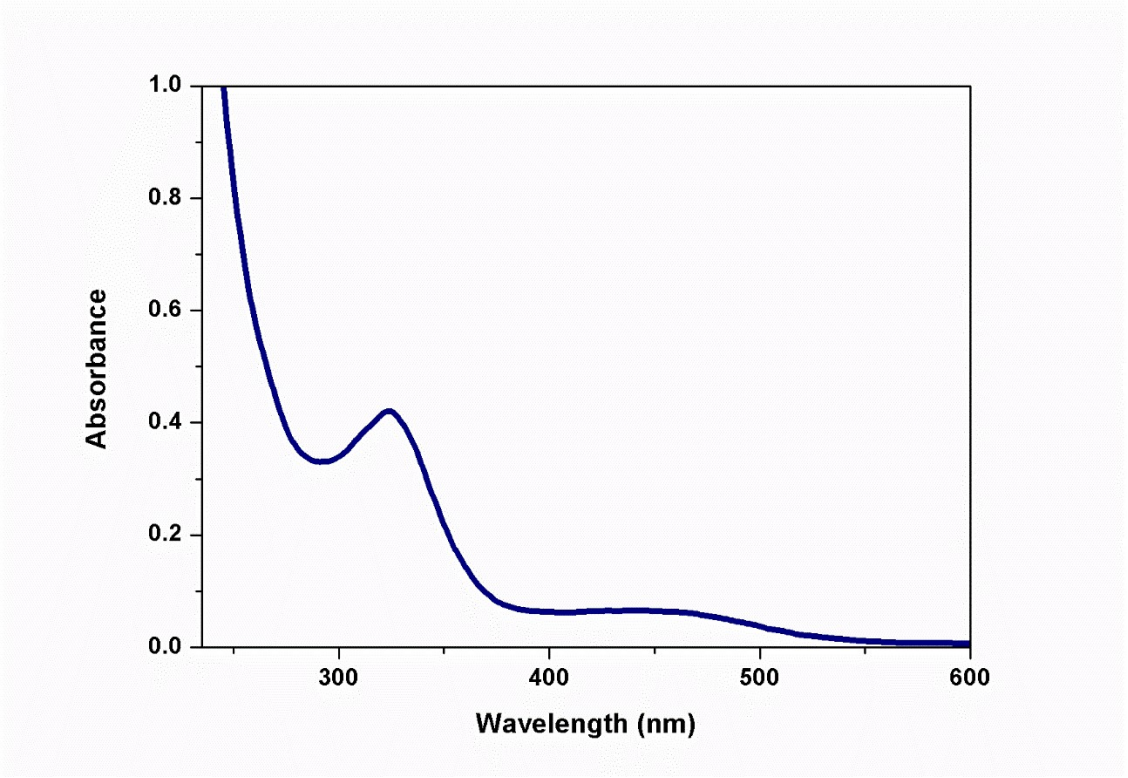

Figure S1. Uv-vis spectrum of complex **Ru_2H1**

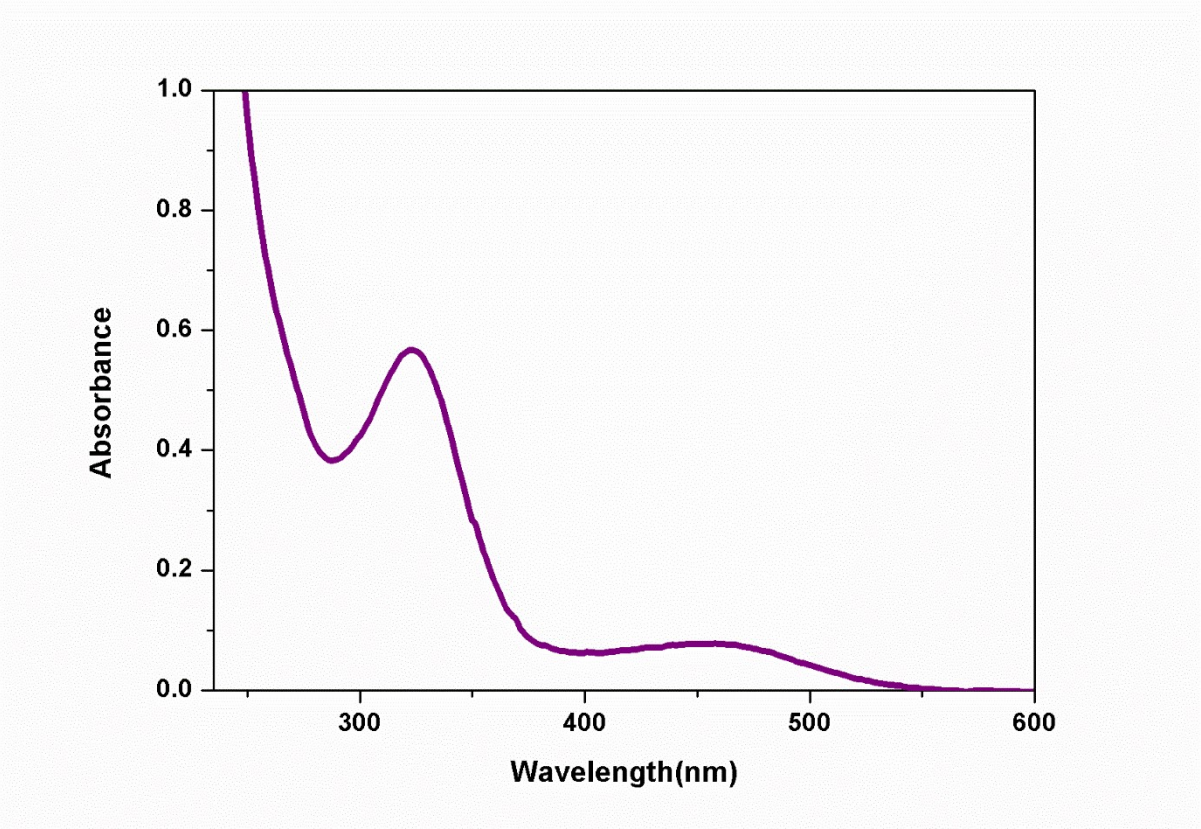

Figure S2. Uv-vis spectrum of complex **Ru_2H2**

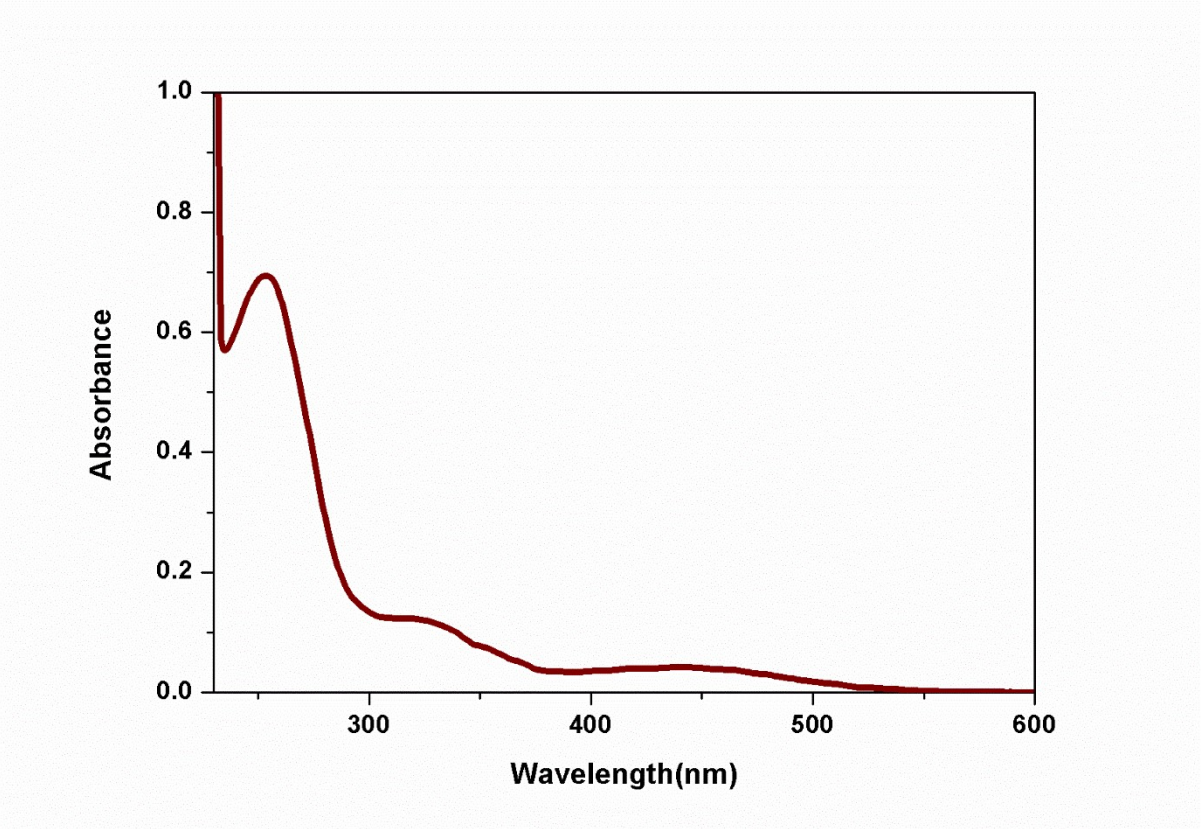

Figure S3. Uv-vis spectrum of complex **Ru_2H3**

4. ^{1}H and $^{13}C\{^{1}H\}$ NMR spectra of the complexes (Ru_2H1- Ru_2H3)

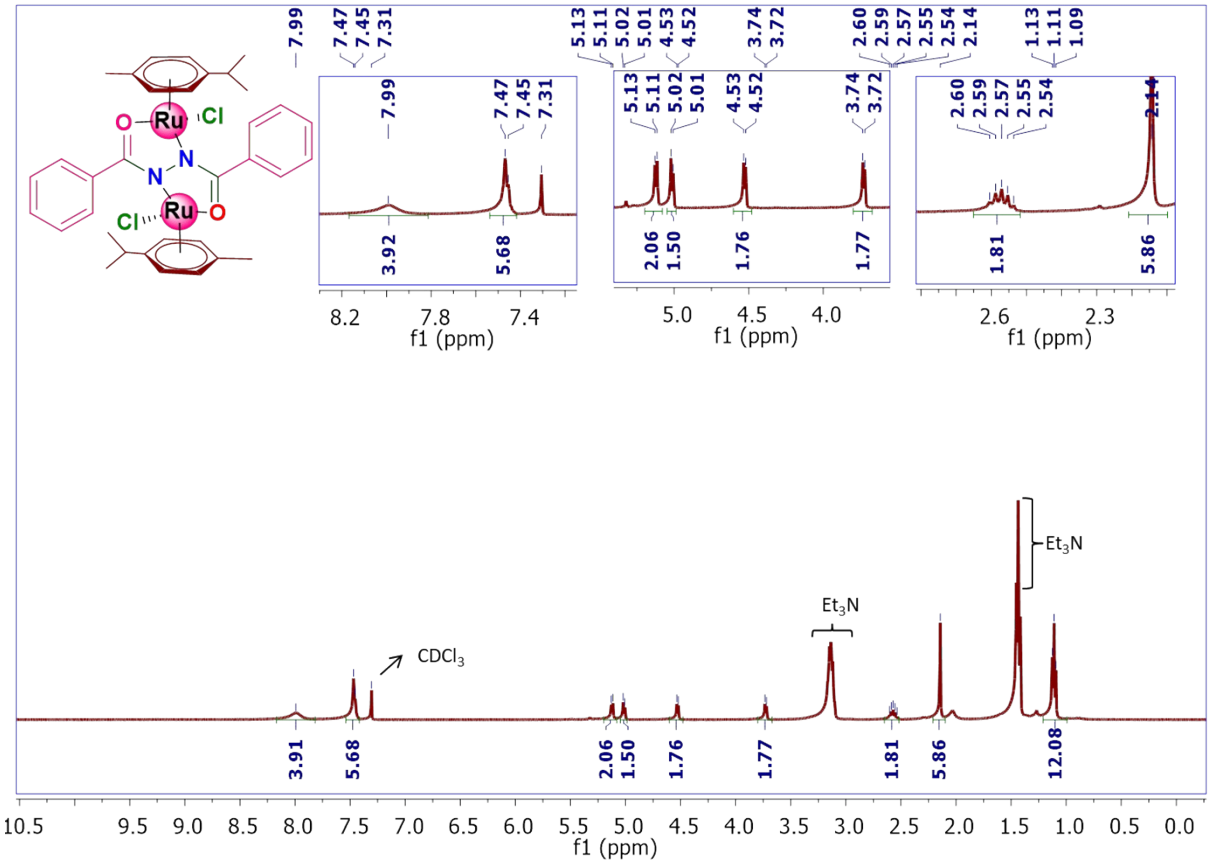

Figure S4.^{1}H NMR spectrum of complex Ru_2H1 in$CDCl_3$ (400 MHz, 293 K).

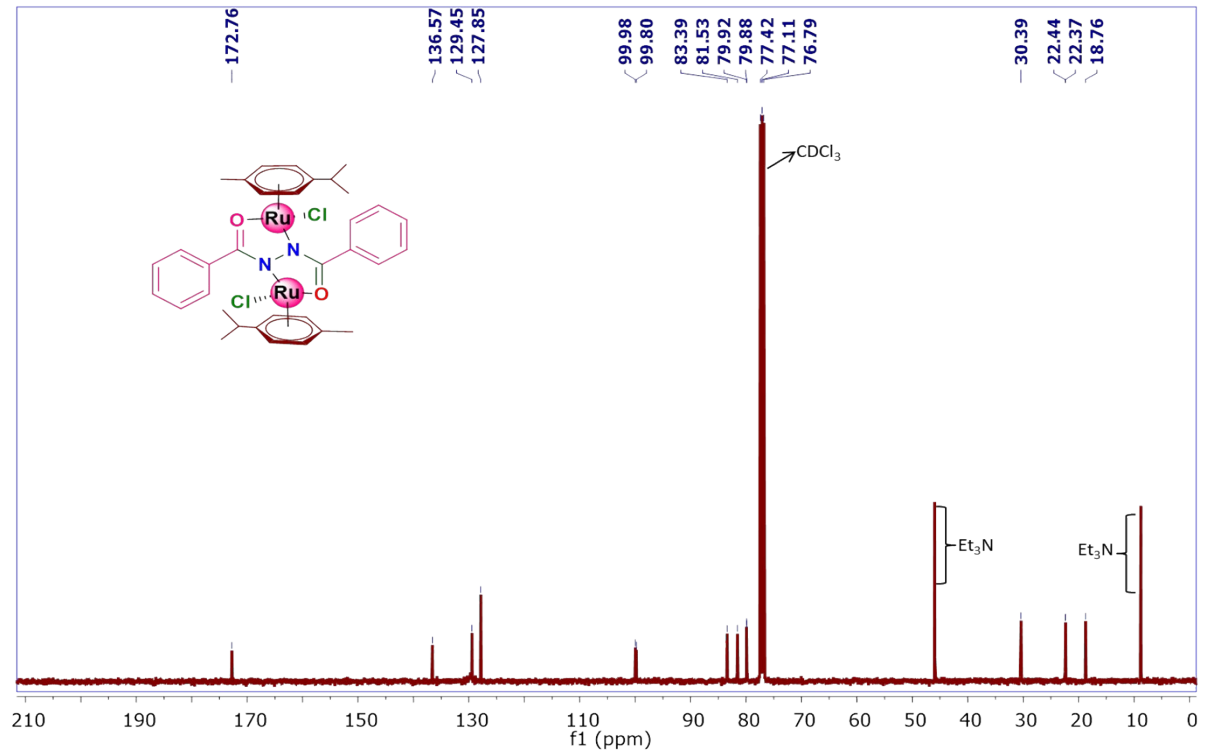

Figure S5. $^{13}C\{^{1}H\}$ NMR spectrum of complex Ru_2H1 in $CDCl_3$ (100 MHz, 293 K).

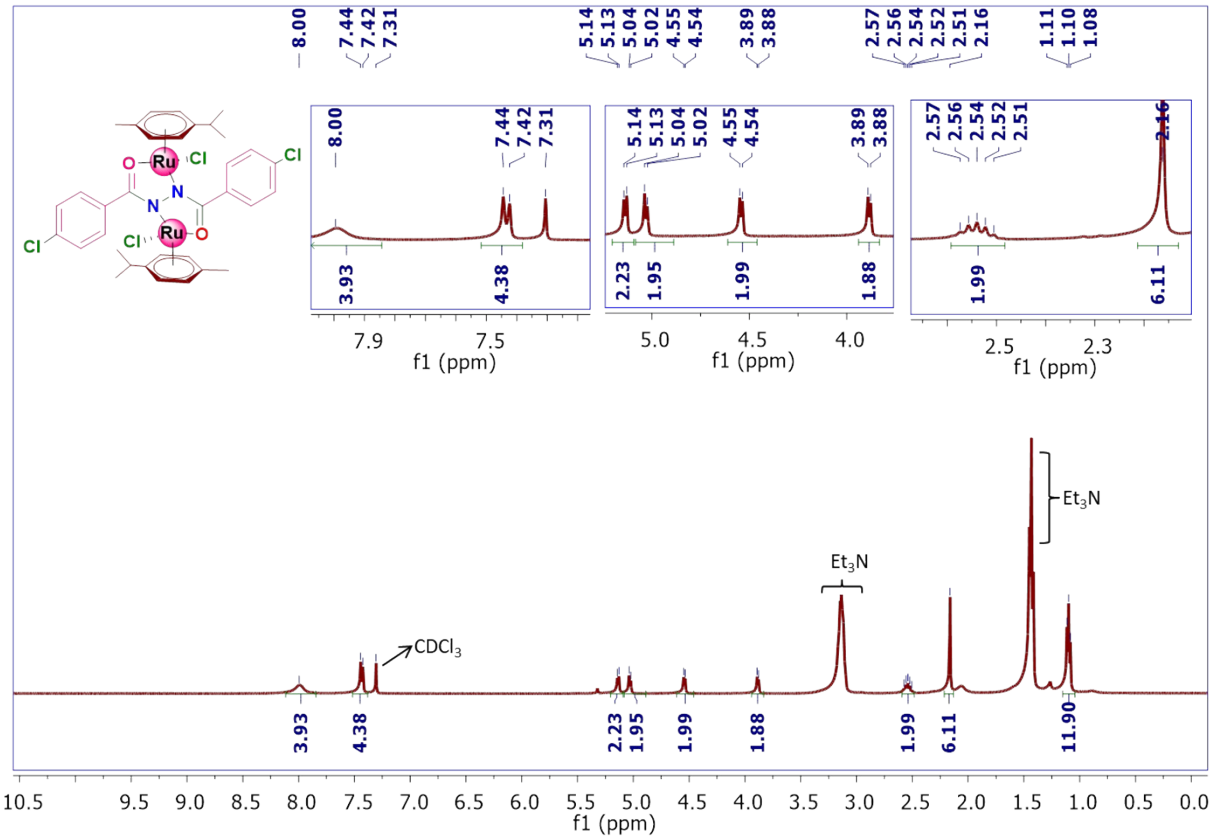

Figure S6. ^{1}H NMR spectrum of complex Ru_2H2 in$CDCl_3$ (400 MHz, 293 K).

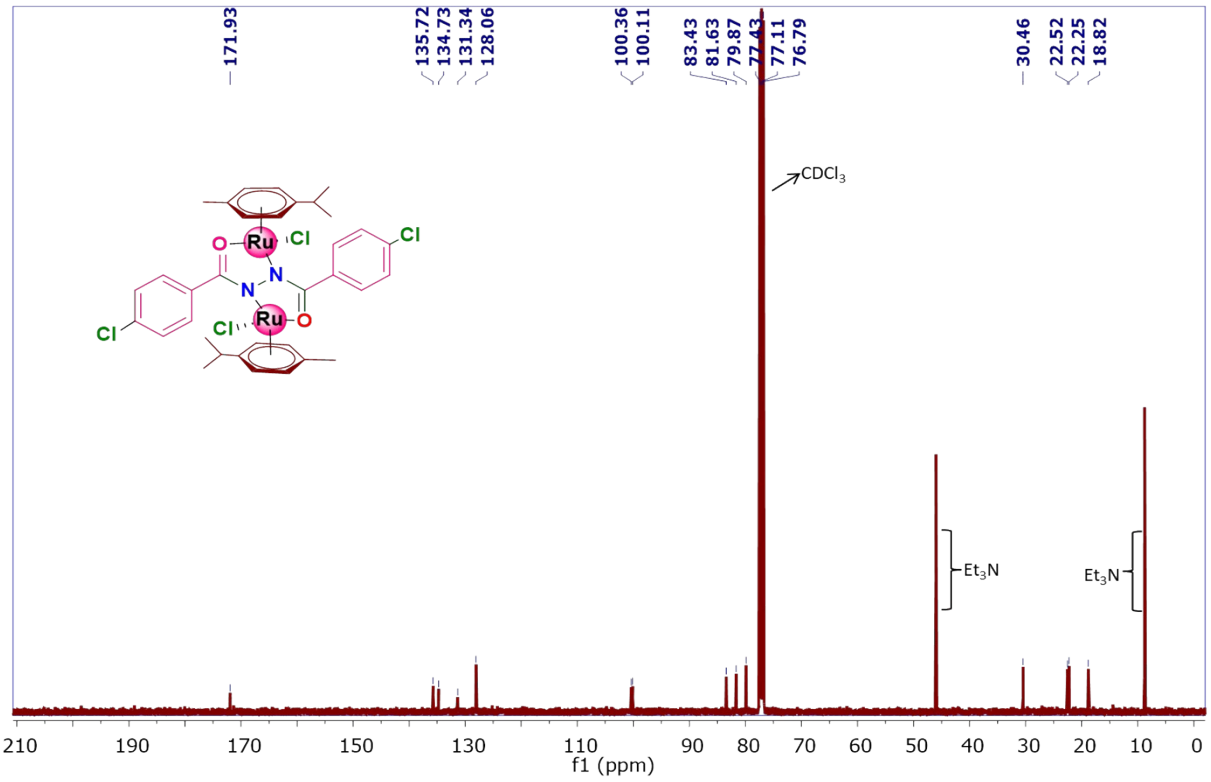

Figure S7. $^{13}C\{^{1}H\}$ NMR spectrum of complex Ru_2H2 in $CDCl_3$ (100 MHz, 293 K).

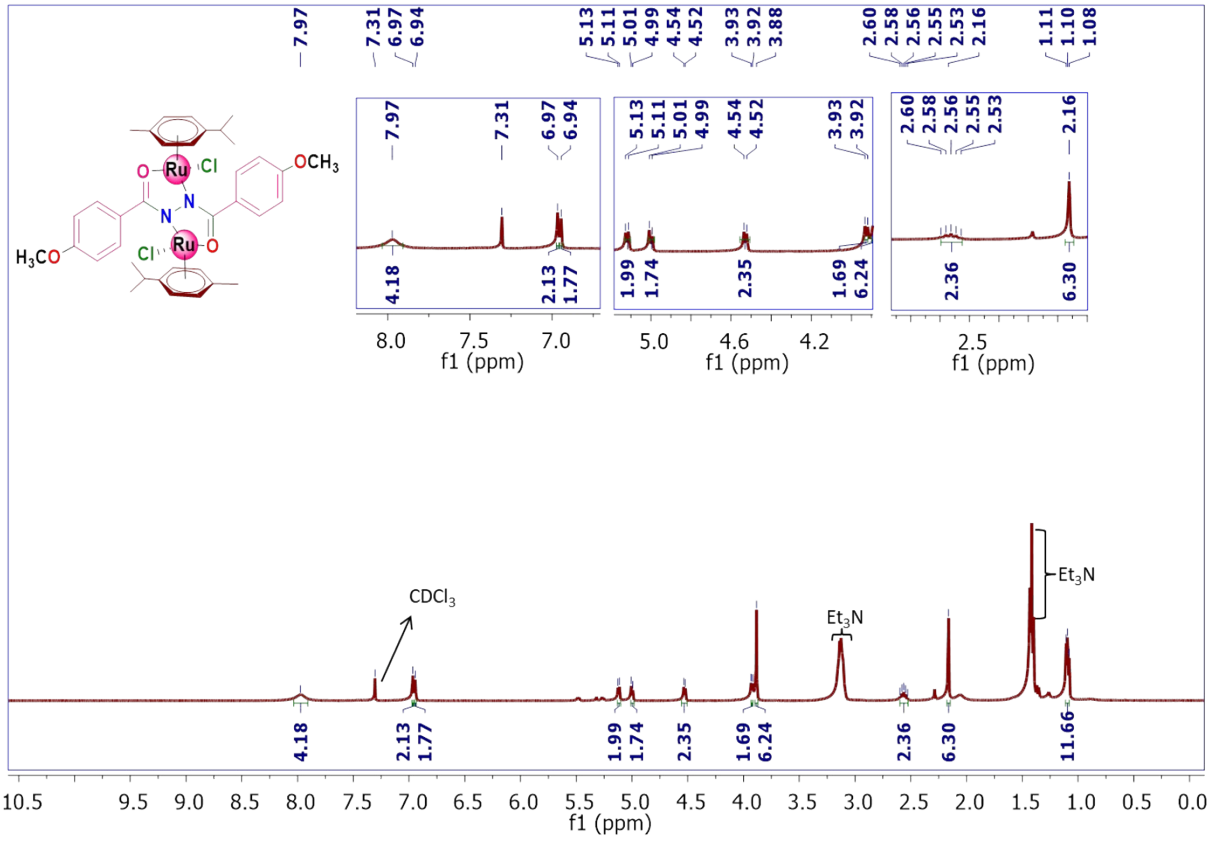

Figure S8. ^{1}H NMR spectrum of complex Ru_2H3 in $CDCl_3$ (400 MHz, 293 K).

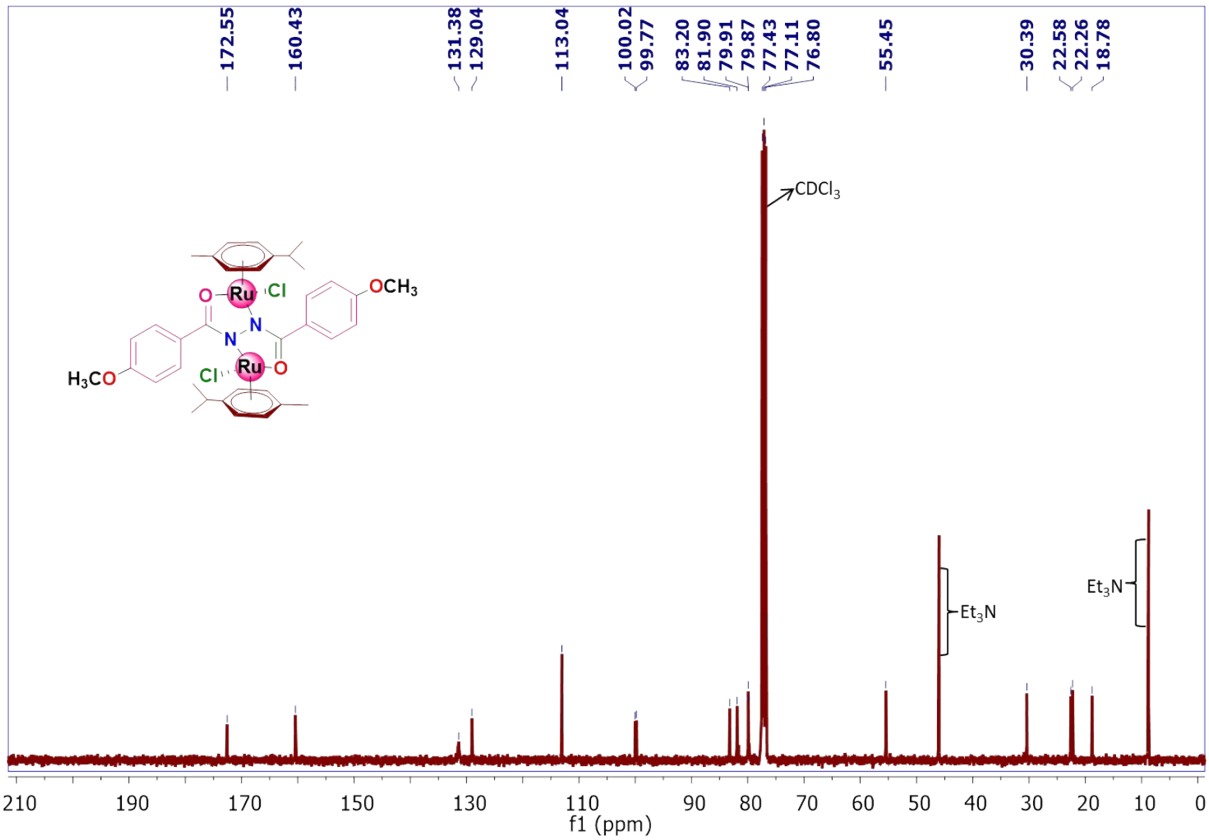

Figure S9. $^{13}C\{^{1}H\}$ NMR spectrum of complex Ru_2H3 in $CDCl_3$ (100 MHz, 293 K).

5. Mass spectra of complexes (Ru_2H1- Ru_2H3)

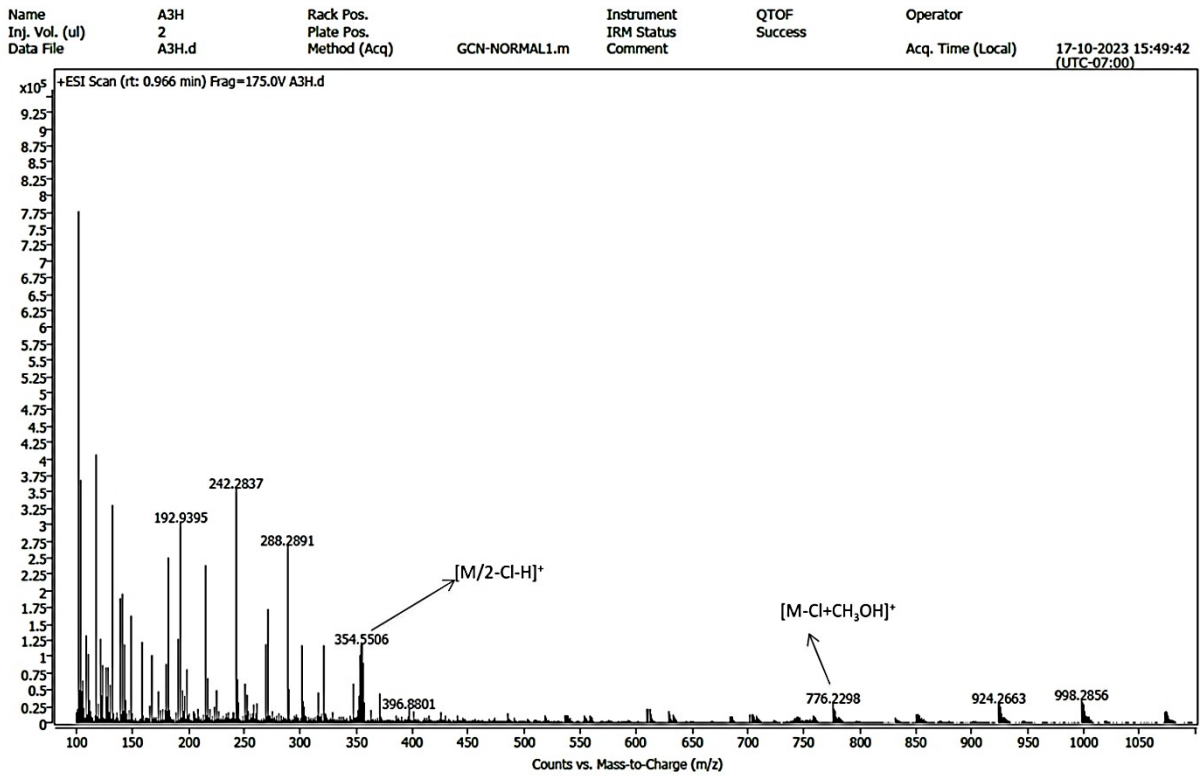

Figure S10. HR-MS spectrum of Ru_2H1

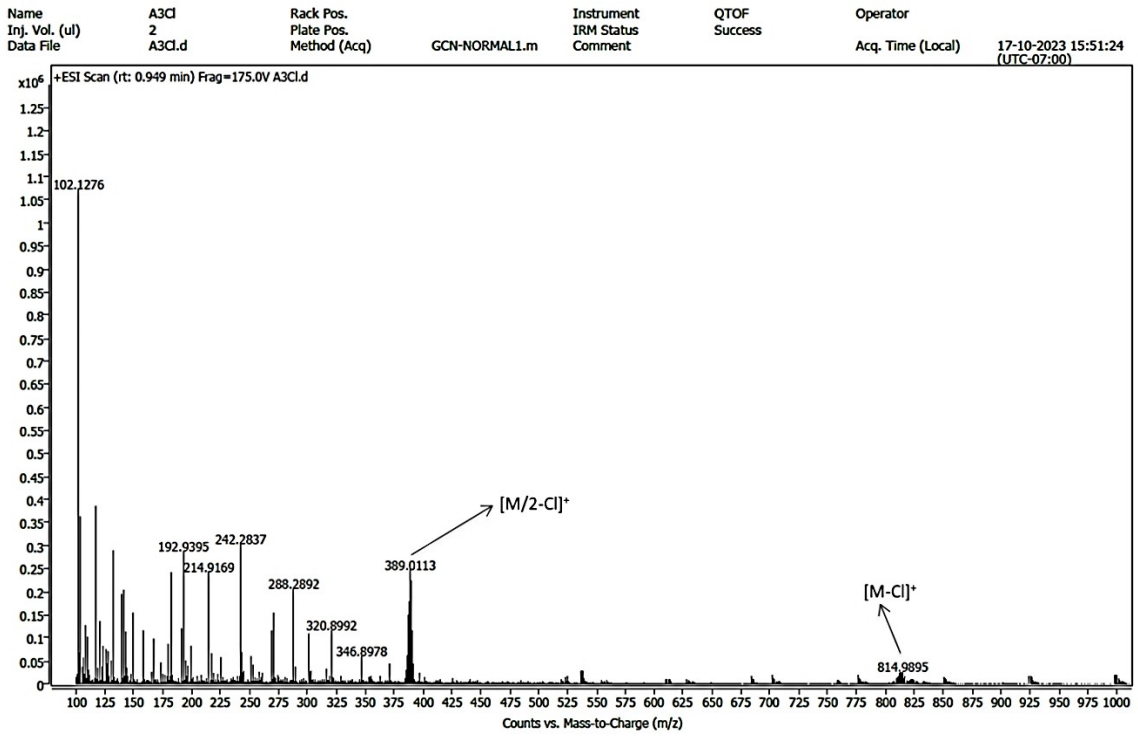

Figure S11. HR-MS spectrum of Ru_2H2

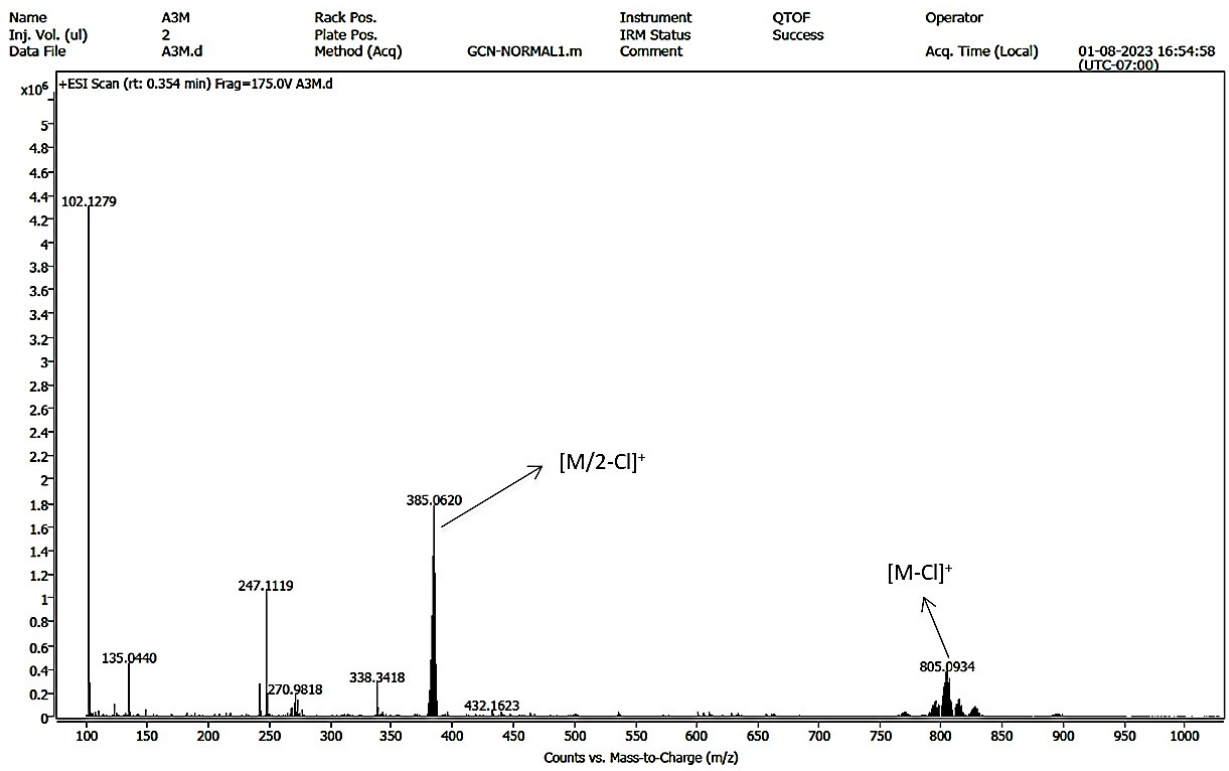

Figure S12. HR-MS spectrum of Ru_2H3

6. Table S1.Crystal data and structure refinement for complexes Ru_2H1 and Ru_2H3

Identification code	Ru_2H1	Ru_2H3
CCDC Number	2181517	2181516
Empirical formula	$C_{34}H_{38}Cl_2N_2O_2Ru_2$	$C_{36}H_{42}Cl_2N_2O_4Ru_2$
Formula weight	779.70	839.75
Temperature/K	295(2)	295(2)
Crystal system	monoclinic	monoclinic
Space group	P21/n	P21/n
a/Å	9.2655(5)	9.0486(4)
b/Å	9.9605(7)	9.7472(7)
c/Å	18.2413(11)	20.1531(11)
α/°	90	90
β/°	96.945(5)	93.009(4)
γ/°	90	90
Volume/Å3	1671.11(19)	1775.03(18)
Z	2	2
ρcalcg/cm3	1.550	1.571
μ/mm-1	1.096	1.042
F(000)	788.0	852.0
Crystal size/mm3	0.38 × 0.15 × 0.04	0.31 × 0.11 × 0.05
Radiation	Mo Kα (λ = 0.71073)	Mo Kα (λ = 0.71073)
2Θ range for data collection/°	7.198 to 58.378	7.232 to 58.534
Index ranges	-8 ≤ h ≤ 12, -9 ≤ k ≤ 13, -22 ≤ l ≤ 23	-11 ≤ h ≤ 9, -13 ≤ k ≤ 9, -27 ≤ l ≤ 25
Reflections collected	8923	9370
Independent reflections	3884 [Rint = 0.0372, Rsigma = 0.0544]	4203 [Rint = 0.0376, Rsigma = 0.0551]
Data/restraints/parameters	3884/0/204	4203/1/212
Goodness-of-fit on F2	1.086	1.062
Final R indexes [I>=2σ (I)]	R1 = 0.0405, wR2 = 0.0814	R1 = 0.0440, wR2 = 0.0919
Final R indexes [all data]	R1 = 0.0621, wR2 = 0.0943	R1 = 0.0861, wR2 = 0.1105
Largest diff. peak/hole / e Å-3	0.62/-0.64	0.54/-0.58

7. Table S2. Selected bond lengths and bond angles for complexes Ru_2H1 and Ru_2H3

Bond length (Å)	**Ru_2H1**
Ru(1)-Cl(1)	2.4118(10)
Ru(1)-N(1)	2.080(3)
Ru(1)-O(1)	2.063(2)
Ru(1)-C(8)	2.211(4)
Ru(1)-C(9)	2.190(3)
Ru(1)-C(10)	2.142(3)
Ru(1)-C(11)	2.189(4)
N(1)-N(1)^1	1.425(5)
C(1)-O(1)^1	1.280(4)
C(1)-N(1)	1.311(4)
Ru(1)-Centroid	1.663
Bond angles (°)	
O(1)-Ru(1)-Cl(1)	85.02(8)
O(1)-Ru(1)-N(1)	76.22(9)
N(1)-Ru(1)-Cl(1)	83.97(8)
N(1)-Ru(1)-C(8)	135.12(13)
N(1)-Ru(1)-C(9)	105.16(13)
C(8)-Ru(1)-Cl(1)	91.23(11)
C(12)-Ru(1)-C(8)	67.87(15)
O(1)^1-C(1)-N(1)	123.3(3)
O(1)^1-C(1)-C(2)	116.1(3)
C(1)-N(1)- N(1)^1	111.9(3)
N(1)-C(1)-C(2)	120.5(3)
C(9)-C(8)-Ru(1)	70.5(2)
C(13)-C(12)-Ru(1)	72.5(2)
C(12)-C(13)-C(8)	120.3(4)
C(13)-C(8)-Ru(1)	70.2(2)
C(16)-C(15)-C(17)	103.6(8)

Bond length (Å)	**Ru_2H3**
Ru(1)-Cl(1)	2.3951(14)
Ru(1)-N(1)	2.094(3)
Ru(1)-O(1)	2.059(3)
Ru(1)-C(9)	2.203(4)
Ru(1)-C(10)	2.174(4)
Ru(1)-C(11)	2.143(4)
Ru(1)-C(12)	2.190(5)
O(1)-C(1)	1.275(5)
N(1)-N(1)^1	1.418(6)
C(1)^1-N(1)	1.303(5)
C(9)-C(15)	1.516(8)
Ru(1)-Centroid	1.664
Bond angles (°)	
O(1)-Ru(1)-Cl(1)	84.32(10)
N(1)-Ru(1)-Cl(1)	84.71(10)
N(1)-Ru(1)-O(1)	75.56(11)
N(1)-Ru(1)-C(9)	143.5(2)
C(12)-Ru(1)-Cl(1)	169.59(13)
O(1)-Ru(1)-C(10)	105.57(17)
C(13)-Ru(1)-Cl(1)	67.30(19)
C(14)-Ru(1)-Cl(1)	106.07(16)
C(12)-C(13)-Ru(1)	73.9(3)
C(9)-C(8)-Ru(1)	72.3(3)
N(1)^1-C(1)-O(1)	123.1(4)
C(2)-C(1)-N(1)^1	121.4(3)
C(8)-O(2)-C(5)	118(4)
C(2)-C(1)-O(1)	115.5(3)
C(10)-C(9)-Ru(1)	70.3(3)
C(9)-C(14)- Ru(1)	72.3(3)

8. Stability studies of the complexes (Ru_2H1- Ru_2H3)

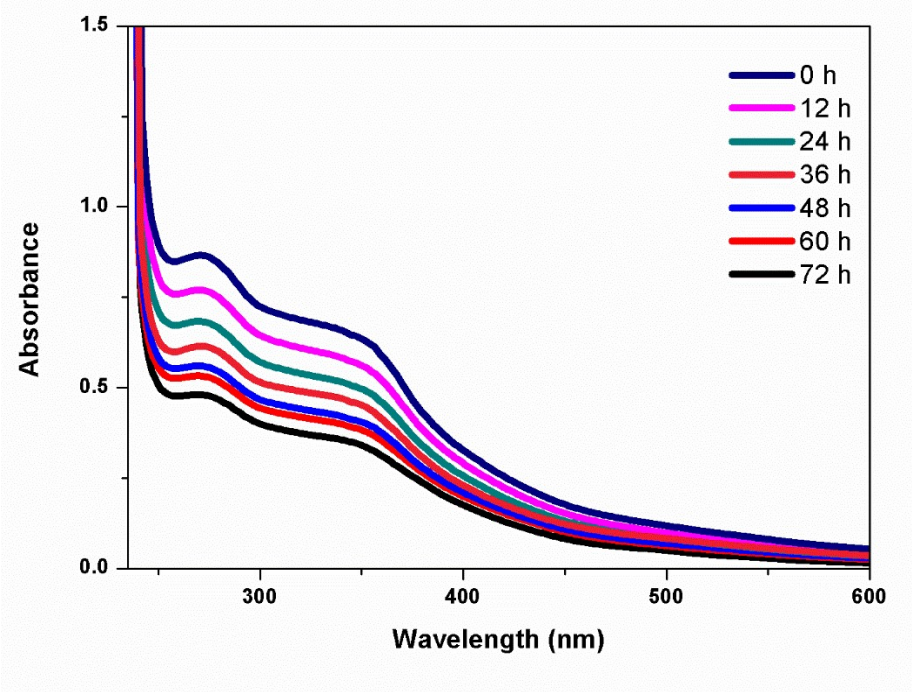

Figure S13. UV-vis spectrum of complex **Ru_2H1** in 1% DMSO in phosphate buffer at 293K over various time intervals (0-72 h)

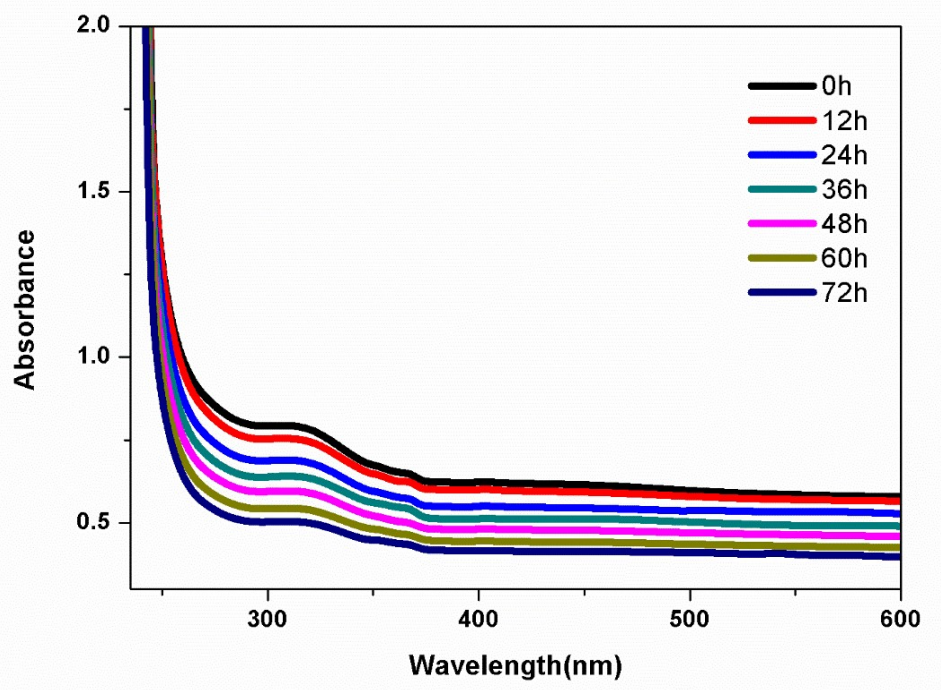

Figure S14. UV-vis spectrum of complex **Ru_2H2** in 1% DMSO in phosphate buffer at 293K over various time intervals (0-72 h)

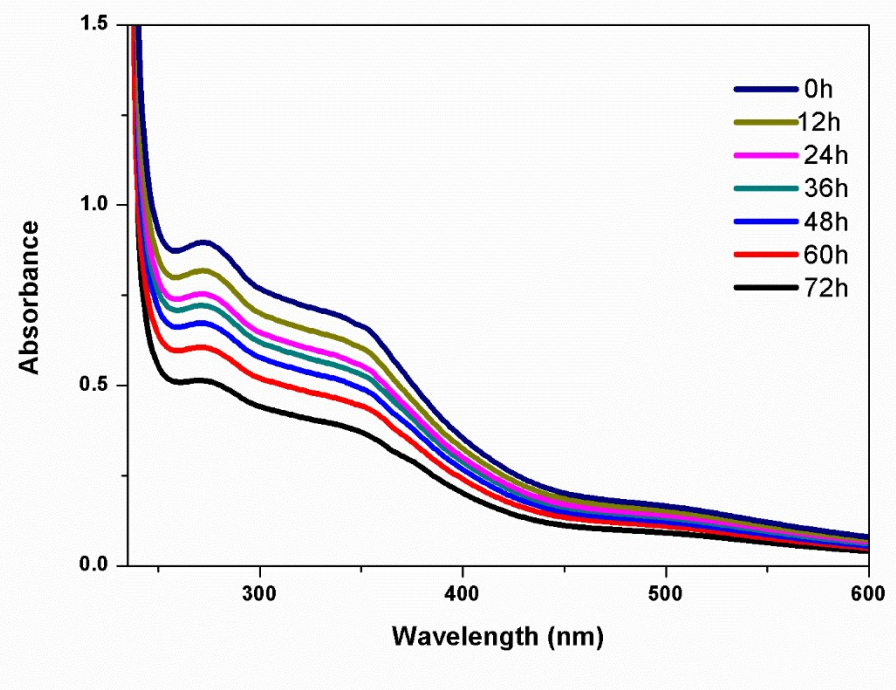

Figure S15. UV-vis spectrum of complex **Ru_2H3** in 1% DMSO in phosphate buffer at 293K over various time intervals (0-72hr).

9. Stability studies of the complex (Ru_2H2) using NMR spectroscopy

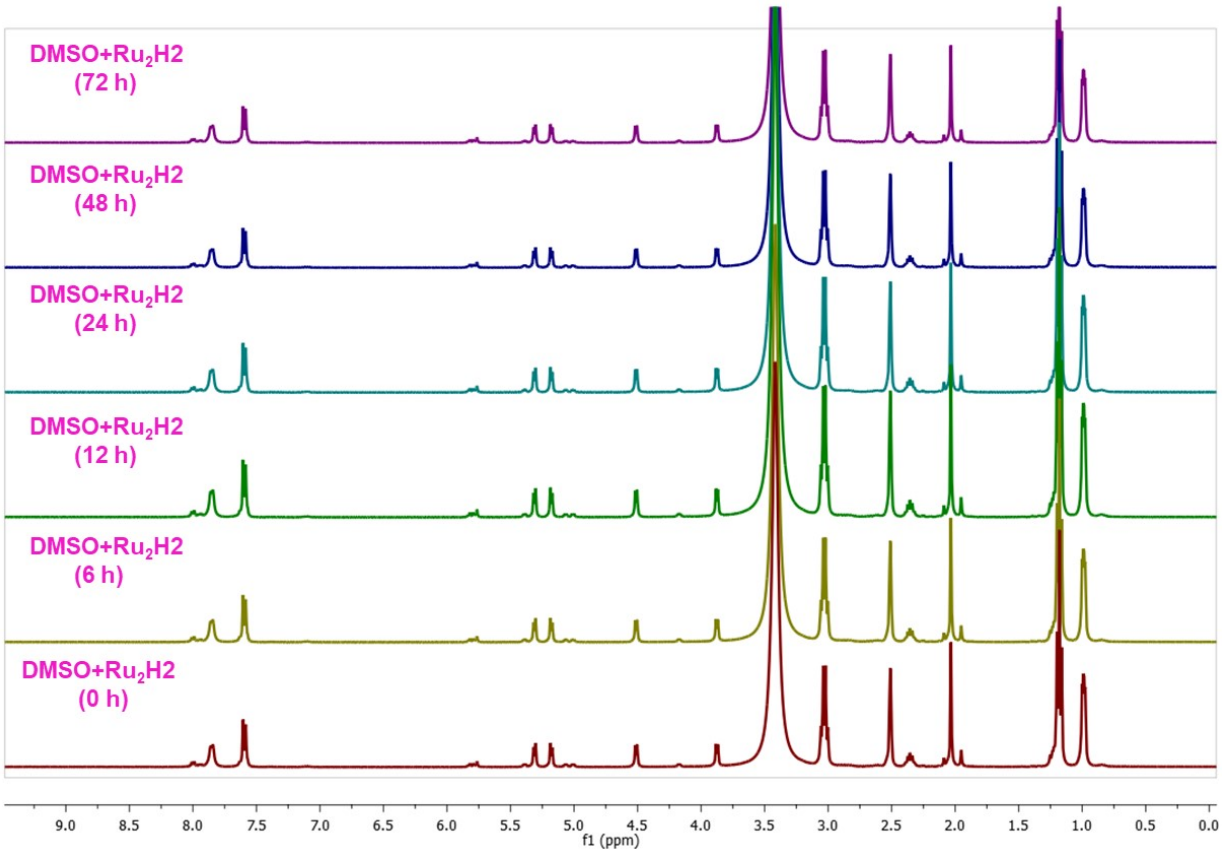

Figure S16. ^{1}H NMR spectra of the complex **Ru_2H2** in DMSO(d_6)over a period of 72 h.

10. Aquation behaviour of the complex Ru_2H2 using NMR spectroscopy

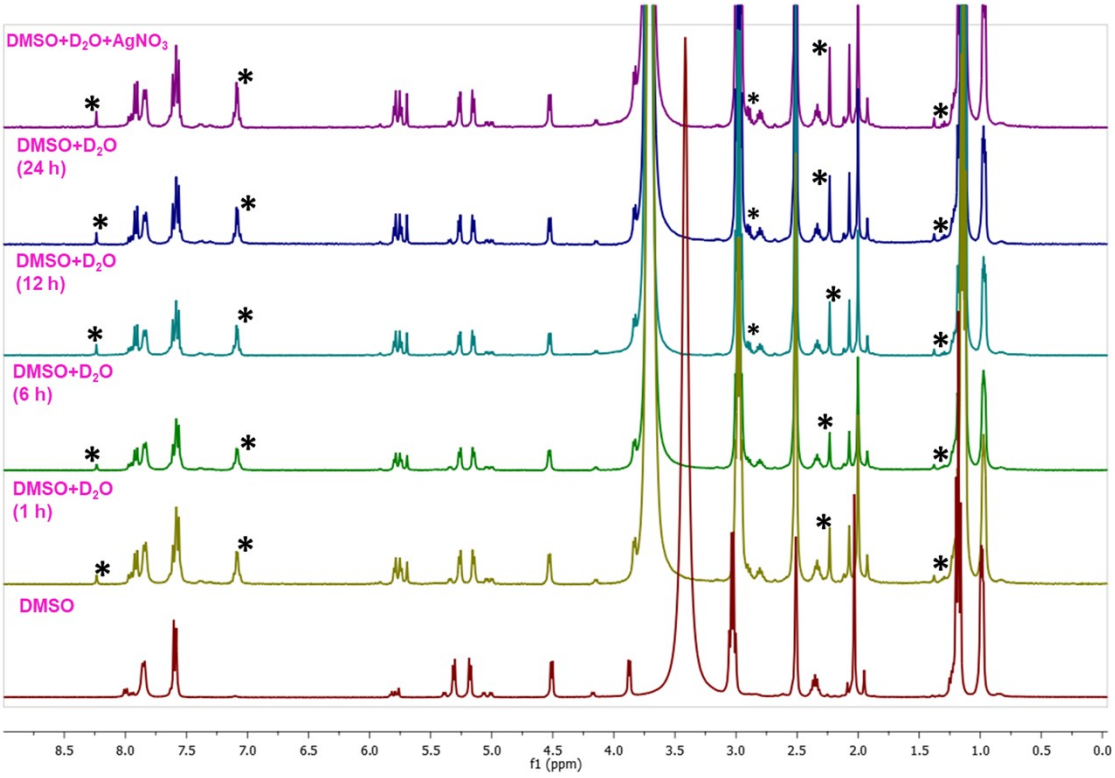

Figure S17. Time-dependent ^{1}H NMR spectra in DMSO(d_6)-D_2O (6:4) mixture of complex **Ru_2H2** over a period of 24 h, and after the addition of $AgNO_3$.

11. Stastical analysis of ligands(HL1-HL3) and complexes (Ru_2H1-Ru_2H3) in cancerous cells

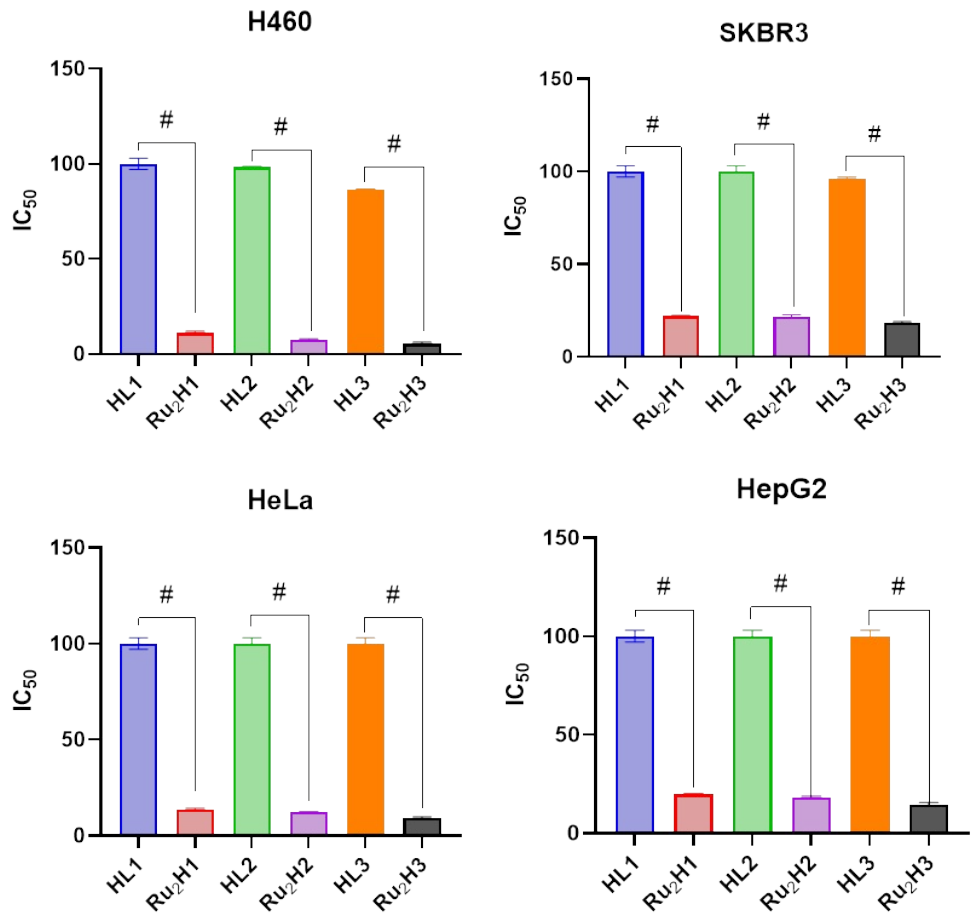

Figure S18. Comparision of ligands(HL1-HL3) and Complexes (**Ru_2H1-Ru_2H3**) using student's t test.

12. References

1. Bennett, M. A.; Smith, A. K. Arene ruthenium (II) complexes formed by dehydrogenation of cyclohexadienes with ruthenium (III) trichloride. *Journal of the Chemical Society, Dalton Trans.* **1974**, *2*, 233-241.
2. Bennett, M. A.; Huang, T. N.; Matheson, T. W.; Smith, A. K.; Ittel, S.; Nickerson, W. *Inorg. Synth*. **1982**, 74.
3. I. Vogel. *Text Book of Practical Organic Chemistry*, fifth ed., Longman, London, **1989**.
4. (a) Sheldrick, GM (1997) SHELXL 97. Program for the Refinement of Crystal Structure, University of Göttingen, Germany. (b) Sheldrick GM (1997) SHELXS 97. Program for Crystal Structure Determinations, University of Göttingen, Germany. (c) Sheldrick, G. M. A short history of SHELX. *ActaCrystallogr*. A, **2008**, *64*, 112-122.
5. Dolomanov, O. V.; Bourhis, L. J.; Gildea, R. J.; Howard, J. A. K.; Puschmann, H.; J. *Appl.Cryst.*, **2009**, *42*,339-341.
6. Farrugia, L. J. ORTEP-3 for Windows-a version of ORTEP-III with a Graphical User Interface (GUI). *J. Appl. Crystallogr*. **1997**, *30*, 565-565.
7. (a) Wang, F.; Chen, H.; Parsons, S.; Oswald, I. D. H.; Davidson, J. E.; Sadler, P. J. Kinetics of Aquation and Anation of Ruthenium(II) Arene Anticancer Complexes, Acidity and X-Ray Structures of Aqua Adducts. *Chem. Eur. J*,.**2003**, *9*, 5810-5820
   (b) Kubanik, M.; Holtkamp, H.; Sohnel, T., Jamieson, S. M.; Hartinger, C. G. Impact of the halogen substitution pattern on the biological activity of organoruthenium 8-hydroxyquinoline anticancer agents. *Organometallics*, **2015**, *34*, 5658-5668. (c) Swaminathan, S.; Haribabu, J.; Subarkhan, M. K. M.; Gayathri, D.; Balakrishnan, N.; Bhuvanesh, N.; Karvembu, R. Impact of aliphatic acyl and aromatic thioamide substituents on the anticancer activity of Ru (II)-p-cymene complexes with acylthiourea ligands- *in vitro* and *in vivo* studies. *Dalton transactions*, **2021**, *50*, 16311-16325.
8. (a) Gupta, R. K.; Sharma, G.; Pandey, R.; Kumar, A.; Koch, B.; Li, P. Z.; Pandey, D. S. DNA/protein binding, molecular docking, and in vitro anticancer activity of some thioether-dipyrrinato complexes. *Inorg. chem*. **2013**, *52*, 13984-13996. (b) Gupta, R. K.; Pandey, R.; Sharma, G.; Prasad, R.; Koch, B.; Srikrishna, S.; Pandey, D. S.; DNA binding and anti-cancer activity of redox-active heteroleptic piano-stool Ru (II), Rh

(III), and Ir (III) complexes containing 4-(2-methoxypyridyl) phenyldipyrromethene. *Inorg. chem.* **2013**, *52*, 3687-3698.